



Highly depleted cratonic mantle in West Greenland extending into diamond stability field in the Proterozoic

Stefan Bernstein^{a,c}, Kristoffer Szilas^{b,c,*}, Peter B. Kelemen^b

^a Avannaq Resources, Dronningens Tværgade 48 st.tv, 1302 Copenhagen K, Denmark

^b Lamont-Doherty Earth Observatory, PO Box 1000, Palisades, NY 10964-8000, USA

^c Natural History Museum of Denmark, Copenhagen University, Øster Voldgade 5-7, 1350 Copenhagen K, Denmark

ARTICLE INFO

Article history:

Received 19 November 2012

Accepted 17 February 2013

Available online 26 February 2013

Keywords:

Greenland

Qeqertaa

SCLM

North Atlantic craton

Dunite

ABSTRACT

This study presents electron microprobe data for dunite xenoliths from a lamprophyre dyke located on the island of Qeqertaa, West Greenland. The minimum age of this dyke is Palaeoproterozoic and it experienced amphibolite facies metamorphism and deformation during that era. The samples consist of nearly 200 xenoliths with a size range of 0.5–8 cm. These dunite xenoliths have olivine Mg#, that range from 80.3 to 94.6 ($n = 579$) with a mean of 92.6. Orthopyroxene is found in three xenoliths and garnet in five others. The latter suggests the depth of the Qeqertaa xenolith suite to be near the diamond stability-field, which is substantiated by the finding of diamonds in bulk samples of the Qeqertaa dyke. This further indicates the presence of a lithospheric mantle domain dominated by high-Mg# dunite to this depth in Palaeoproterozoic time. Cr-rich spinel, in the 0.1–0.2 mm size range, is found within and between olivine grains in individual xenoliths. These Cr-spinels yield Fe–Mg exchange temperatures of 400–600 °C. However, the presence of intermediate spinel compositions spanning the lower temperature solvus suggests that equilibration temperatures were >550 °C. $Fe^{3+}\#$, expressed as $100 \times Fe^{3+}/(Fe^{3+} + Al + Cr)$, is shown to be a useful parameter in order to screen for altered spinel ($Fe^{3+}\# > 10$) with disturbed Mg# and Cr#. The screened spinel data ($Fe^{3+}\# < 10$) show a distinctly different trend in terms of spinel Cr# versus Mg#, compared to unmetamorphosed xenoliths in Tertiary lavas and dikes from Ubekendt Ejland and Wiedemann Fjord, respectively, also located within the North Atlantic craton. This difference likely reflects amphibolite facies metamorphic resetting of the Qeqertaa xenolith suite by Fe–Mg exchange. Given the similarity of the Qeqertaa xenolith suite with the Ubekendt and Wiedemann suites, in terms of their olivine Mg# and spinel Cr# distribution, high-Mg# dunite is likely to be an important component of the subcontinental lithospheric mantle beneath the North Atlantic craton and appears to have spanned a vertical distance of at least 150 km in this region, even during the Palaeoproterozoic.

© 2013 Elsevier B.V. All rights reserved.

1. Introduction

Determining the composition of the subcontinental lithospheric mantle (SCLM) has implications for our understanding of the crust–mantle system and its evolution through time. Previous studies on SCLM xenoliths from Greenland have shown the occurrence of nearly monomineralic dunitites consisting of remarkably refractory olivine with molar $Mg/(Mg + Fe^{2+})$, or Mg#, averaging about 92.8 (e.g. Bernstein et al., 1998, 2006; Bizzarro and Stevenson, 2003; Garrit, 2000; Wittig et al., 2008). The Qeqertaa xenolith suite presented in this study shows equally refractory olivine compositions. This growing body of data on cratonic mantle xenoliths from Greenland suggests that such olivine-rich mantle is common here, and perhaps comprises a large proportion of the lithospheric mantle beneath substantial parts of Greenland.

High and consistent Mg# in olivine is thought to reflect partial melting of the mantle to the point of exhaustion of orthopyroxene (Bernstein et al., 2007). The implied high degree of melting (37–45%; Bernstein et al., 1998; Herzberg, 2004) is not achieved in any current geological environment and is thus thought to reflect a hotter mantle during the formation of cratonic SCLM. This is in agreement with the generally Archaean Re-depletion ages of cratonic SCLM xenoliths (e.g. Hanghøj et al., 2001; Pearson et al., 2003; Shirey and Walker, 1998; Wittig et al., 2010) and the inferred hotter mantle at that time (Herzberg et al., 2010). However, the exact formation environment is still debated with one model proposing a single-stage process in a polybaric melting column either in a spreading ridge or plume environment (e.g. Aulbach et al., 2011; Bernstein et al., 1998, 2006; Griffin et al., 2009; Herzberg et al., 2010; Kelemen et al., 1998), whereas another model proposes flux melting of previously depleted harzburgite in a subduction zone setting (e.g. Canil, 2004; Lee, 2006; Wittig et al., 2008).

In addition to documenting the composition of the Palaeoproterozoic xenolith suite at Qeqertaa this study also shows that although parameters such as Mg#, and molar $Cr/(Cr + Al)$, or Cr#, may at first appear

* Corresponding author.

E-mail address: kszilas@ldeo.columbia.edu (K. Szilas).

to retain information of the primary composition of a mantle xenolith suite, examination of molar $\text{Fe}^{3+}/(\text{Cr} + \text{Al} + \text{Fe}^{3+})$, or $\text{Fe}^{3+\#}$, in associated spinels reveals a history of alteration that strongly modified both Mg# and Cr# so that even visually unaltered spinel had its chemistry overprinted during amphibolite facies metamorphism. Thus, spinel compositions, which are widely thought to be reliable indicators of primary igneous conditions in metamorphic intrusive rocks (e.g. Barnes, 2000) may reflect re-equilibration during metamorphic events (Evans and Frost, 1975; Sack and Ghiorso, 1991).

2. Geology

The Qeqertaa xenolith suite is hosted by an up to 6 m wide vertical dyke of ultramafic lamprophyric affinity, which crops out on the small island Qeqertaa, some 50 km north of Ilulissat at 69°38' N, 50°38' W (Fig. 1). The dyke is one of many that cut late Archaean gneisses and supracrustal rocks in the Ataa area, eastern Disko Bay (Garde and Steenfelt, 1999; Larsen and Rex, 1992; Marker and Knudsen, 1989). The Qeqertaa dyke has not been dated, but similar intrusions in the Ataa area have yielded K–Ar ages of 1782 Ma and 1743 Ma, both ± 70 Ma (Larsen and Rex, 1992). Because the dykes have been affected both by metamorphism and deformation linked to the Palaeoproterozoic Rinkian–Nagsoqtuqidian orogeny, these ages could represent metamorphic overprinting and thus represent minimum ages, as pointed out by Larsen and Rex (1992). Structural interpretation suggests that the Ataa region can be divided into a series of crustal blocks with distinct tectono-magmatic history (Garde and Steenfelt, 1999) and the Qeqertaa dyke is situated in the border zone between the Ataa domain to the north and the Rodebay domain to the south.

The Qeqertaa xenoliths are rounded to subangular, with a size range of 0.5 cm to 8 cm in the longest dimension. In several places along the dyke, the xenoliths are so abundant as to make a clast-supported network. The dyke has brecciated contacts with tonalitic gneisses, and is deformed with pinch and swell structures. Apophyses are often sheared

into tight isoclinal folds. Deformation mainly affected the matrix, which often shows carbonate crystallization in pressure shadows of the xenoliths and matrix foliation wrapping around individual xenoliths (Fig. 2). Matrix mineralogy is dominated by tremolite, mica, carbonate, ilmenite and iron oxides. Of these minerals, only mica and ilmenite are thought to remain from the primary mineralogy of the dyke matrix, although even these minerals show evidence of alteration and recrystallization, manifested as oxide exsolution along cleavage planes in mica, and exsolution lamellae and oxidized microcrystalline overgrowth zones on ilmenite.

A collection of nearly 200 xenolith samples forms the basis of this study. Individual xenoliths larger than about 3 cm were cut into several slices 5–8 mm thick and all xenoliths were inspected visually before a subset of 119 xenoliths of varying size was prepared for standard polished thin sections and analyzed by electron microprobe. The xenolith suite as a whole appeared very homogeneous in terms of mineral mode, texture and grain size. The xenoliths are all dunites with only a few samples containing spinel, garnet, mica or orthopyroxene (see below). A few xenoliths are completely serpentinized, while others are relatively fresh peridotite with only local alteration along minor cracks and veins. However, as shown below, all studied xenoliths have experienced some degree of chemical modification of their primary minerals even though they at a first glance appear nearly unaltered. Typically, in standard thin sections olivine grain margins are yellowish to light brown, in some samples more dusty brown (Figs. 2 and 3). Such margins can be relatively wide (1–2 mm), but are mostly in the order of 0.2–0.6 mm, such as in the example of xenolith sample qq-2 in Fig. 3. Spinel is often oxidized, with irregular grain margins and is opaque in standard thin sections. In rare cases, the spinel has retained a brownish translucent core. Secondary oxide, mainly magnetite, is common along veins and cracks within olivine grains and at the rim of individual xenoliths (Fig. 3). Some examples of xenoliths and their textures are given in Fig. 2a–d.

All xenoliths are coarse protogranular, following the terminology of Mercier and Nicolas (1975). Grain size varies from 1 to 2 mm to

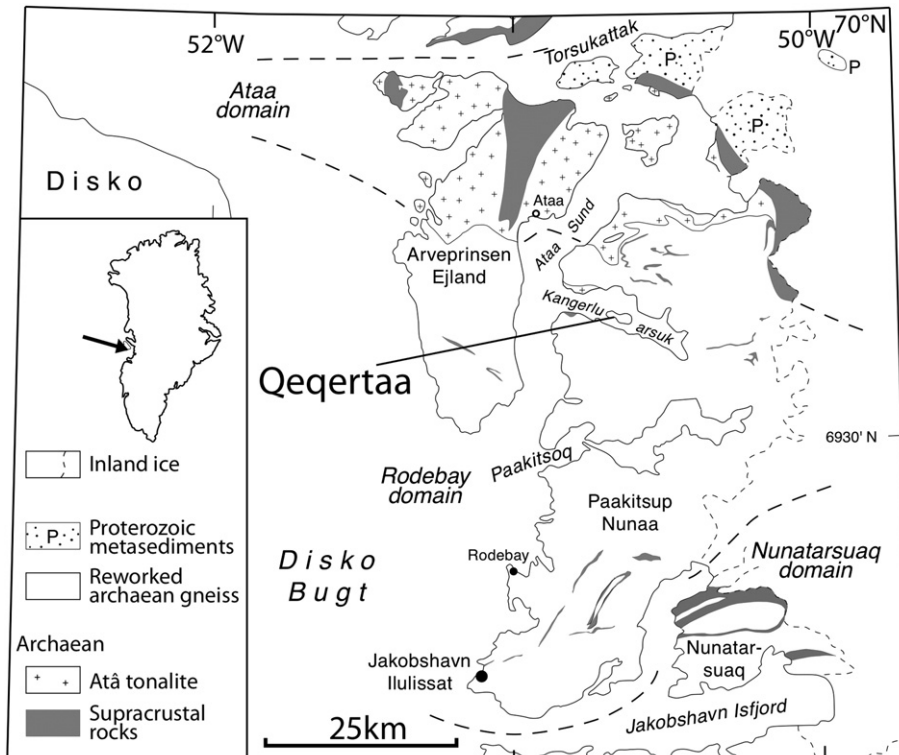


Fig. 1. Simplified geological map over the north-eastern Disko Bay region, showing the location of the island Qeqertaa in the northern Rodebay domain. Qeqertaa is situated a few kilometers south of the border of the Atâ tonalite. After Garde and Steenfelt (1999).

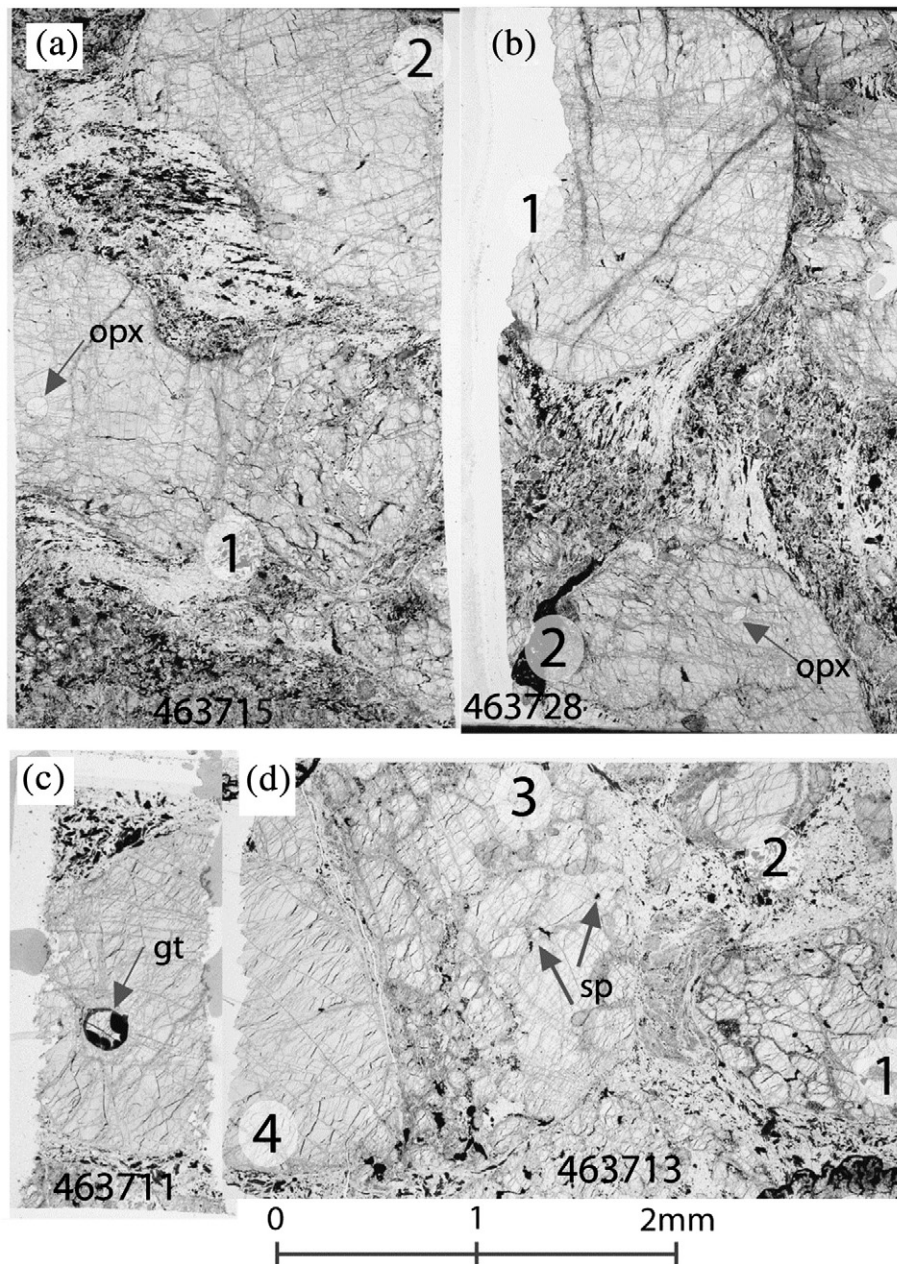


Fig. 2. Examples of xenoliths and olivine megacrysts in the Qeqertaa xenolith suite. a) Sample #463715 xenoliths #1 and #2. Note lobate olivine xenolith (#1) with small (1 mm) rounded orthopyroxene inclusion and right hand side of xenolith fractured by carbonate-Fe-oxide veins. b) Sample #463728 showing spherical dunite xenoliths with small (<1 mm) orthopyroxene inclusion in xenolith #2. Note the carbonate (colorless mineral) filled pressure shadows between the two xenoliths. c) Sample #463711 with rounded garnet inclusion in dunite. Olivine grain is > 20 mm. Garnet partly replaced by kelyphite. d) Sample #463713, showing typical dense clustering of small xenoliths. Xenolith #3 contains small spinel grains (0.1 mm), while the xenoliths #1, #2, and #4 are monomineralic dunite, apart from alteration minerals. Note darker (brown) olivine margins in xenolith #1.

> 30 mm for olivine. Representative smaller xenoliths are composed of only a few olivine grains. Well-rounded olivine megacrysts up to 30 mm are frequently found in the matrix. An example of one coarse grained xenolith is given in Fig. 3, with olivine grain size ranging 1–15 mm. Orthopyroxene, found in three xenoliths, occurs as ~1 mm wide circular inclusions in large olivine grains (Fig. 2). Garnet, found in five xenoliths (out of 200), occurs as rounded 1–2 mm grains, but one 4 mm rounded garnet grain appears in xenolith #463737-1. Only one garnet is partly preserved (sample #463711), while all other grains have been completely replaced by kelyphite (Fig. 2c). Cr-rich spinel is found as minute anhedral inclusions in the 0.1–0.2 mm size range within olivine, or between olivine grains. Relic brown translucent spinel is sometimes found, jacketed by opaque oxide, and nearly always with a thin (20–50 μm wide) coating of mica forming the outer contact to host olivine (Figs. 6a, 7a, 8a). Chrome-bearing magnetite occurs throughout

the xenoliths, as irregular larger grains (1–2 mm), possibly replacing primary chrome spinel. It also occurs as smaller individual grains or aggregates of smaller grains (0.1–0.3 mm), often associated with fractures or veins in olivine. These chrome bearing magnetite grains likely represent alteration products. Primary mica is found in two xenoliths. In sample #463707-2, a 2 mm long colorless mica grain is enclosed by olivine. In sample #463706-3 similar colorless mica is found interstitially to medium grained olivine crystals.

Several xenoliths show evidence of fracturing, and the presence of carbonate–magnetite intergrowths in such fractures suggests that the xenoliths became disaggregated within the lamprophyre dyke during crustal deformation. This can be appreciated in Fig. 2a, showing secondary carbonate mineralization along extensive fracturing of olivine in xenolith #1 in sample #463715 connected to similar carbonate-Fe-oxide intergrowth in the matrix. Another example of this is presented in

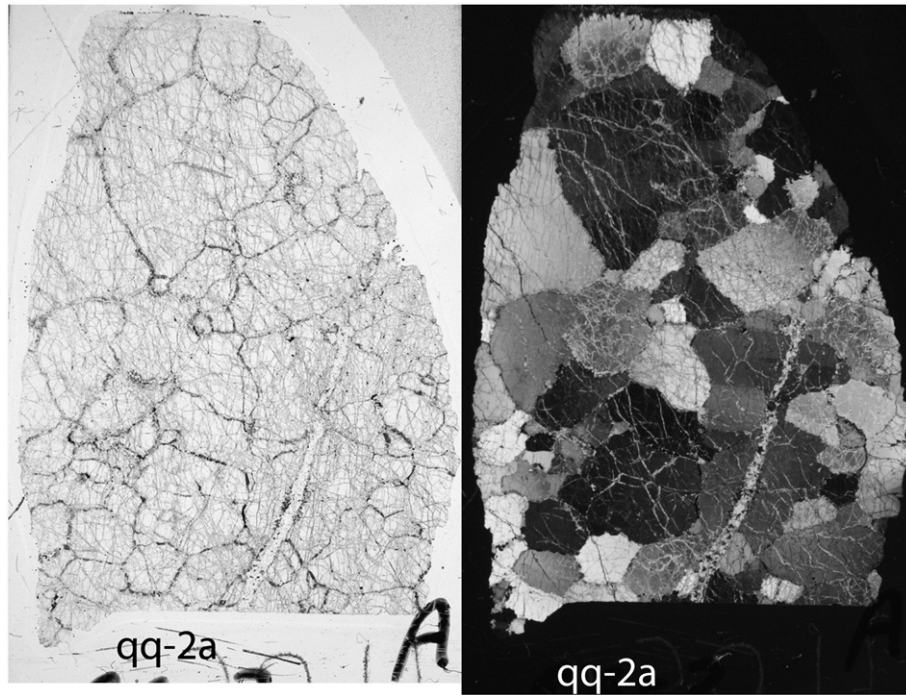


Fig. 3. Xenolith qq-2 with typical coarse, protogranular texture demonstrating the lack of foliation or preferred orientation of the olivine grains (a) plane-polarized light; b) crossed-polarized light). The grain size range for olivine is large, from 2 mm to more than 15 mm. The sample also illustrates the nearly monomineralic nature of the xenolith suite from Qeqertaa.

Fig. 2b (sample #463728), where carbonate-Fe-oxide intergrowth forms 'horns' at the edges of xenoliths #1 and #2 – probably representing growth in pressure shadows.

Tremolite and talc coexist with olivine in some of the altered portions of the xenoliths and provides evidence for premetamorphic alteration of at least parts of the olivine grains. A collection of micro- and macrodiamonds has been recovered from several bulk samples of the Qeqertaa dyke (Marmo et al., 2012) during exploration activities from 2007 to 2012.

3. Analytical technique

Mineral grains were analyzed on standard 40 μm polished thin sections, using the JEOL electron microprobe at the Institute of Geology and Geography, University of Copenhagen. All elements in silicates were measured by WDS, with 20 s peak count time for Na, Mg, Fe, Si, and Ti, while Cr, Ni, Ca and Al were measured with 40 s peak count time. Natural and synthetic standards were measured at the beginning and at the end of each session. For traverses in spinel, an analytical routine optimized for oxides was utilized and the elements analyzed were Mg, Fe, Si, Ca, Ti, Cr, Mn, Fe, Ni and Zn. Peak count time for Zn was 40 s and 10 s for remaining elements. Background count time on either side of the peak was half that of peak count time for both silicates and spinels. Table 1 in the online supplementary material lists a series of representative mineral data. The mineral data presented there represents the core compositions, typically 2–3 analyses, and for orthopyroxene and garnet, an average of 4–6 analyses.

4. Results

4.1. Olivine chemistry

There is a large compositional variation in olivine. The overall range in Mg# ($100 \times \text{Mg}/(\text{Mg} + \text{Fe}^{2+})$) out of almost 600 analyses is from 80.3 to 94.6 as shown in the insert in Fig. 4. Ni varies from 1328 ppm to 4008 ppm (median value of 2727 ppm) and does not

correlate with Mg#. Because olivine composition cannot be related to the textural state of olivine, i.e. xenocrystic or xenolithic (not shown), all olivine in the following is referred to as xenoliths. Fig. 4 also shows the distribution of Mg# in olivine in 119 individual xenoliths, as presented in Table 1 (see online supplementary material). While this data set represents core compositions, the range in Mg# is similarly large, spanning Mg# 80–94. Neither of the data sets (all olivine analyses and xenolith cores only) show a good correlation of Ni versus Mg# (see Fig. 4, insert). Several olivine grains have been analyzed along traverses from crystal rim to core. The data are presented in Fig. 5 in terms of the variations in Mg# and Ni contents. Fig. 5a shows a traverse over about 0.3 mm in the core of a large olivine crystal. The variation in Mg# is moderate in the range 93.4–94.1, while Ni is in the range 2295–2955 ppm. These ranges are only slightly larger

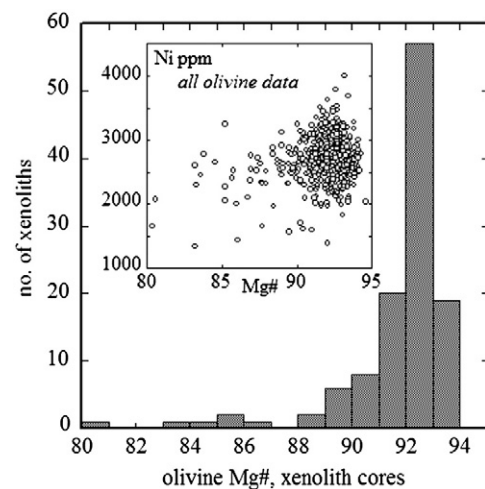


Fig. 4. Range in olivine compositions as reflected by Mg# ($100 \times \text{Mg}/(\text{Mg} + \text{Fe}^{2+})$) and Ni content in ppm. Histogram shows data for 119 individual olivine xenoliths, while insert shows all olivine analyses.

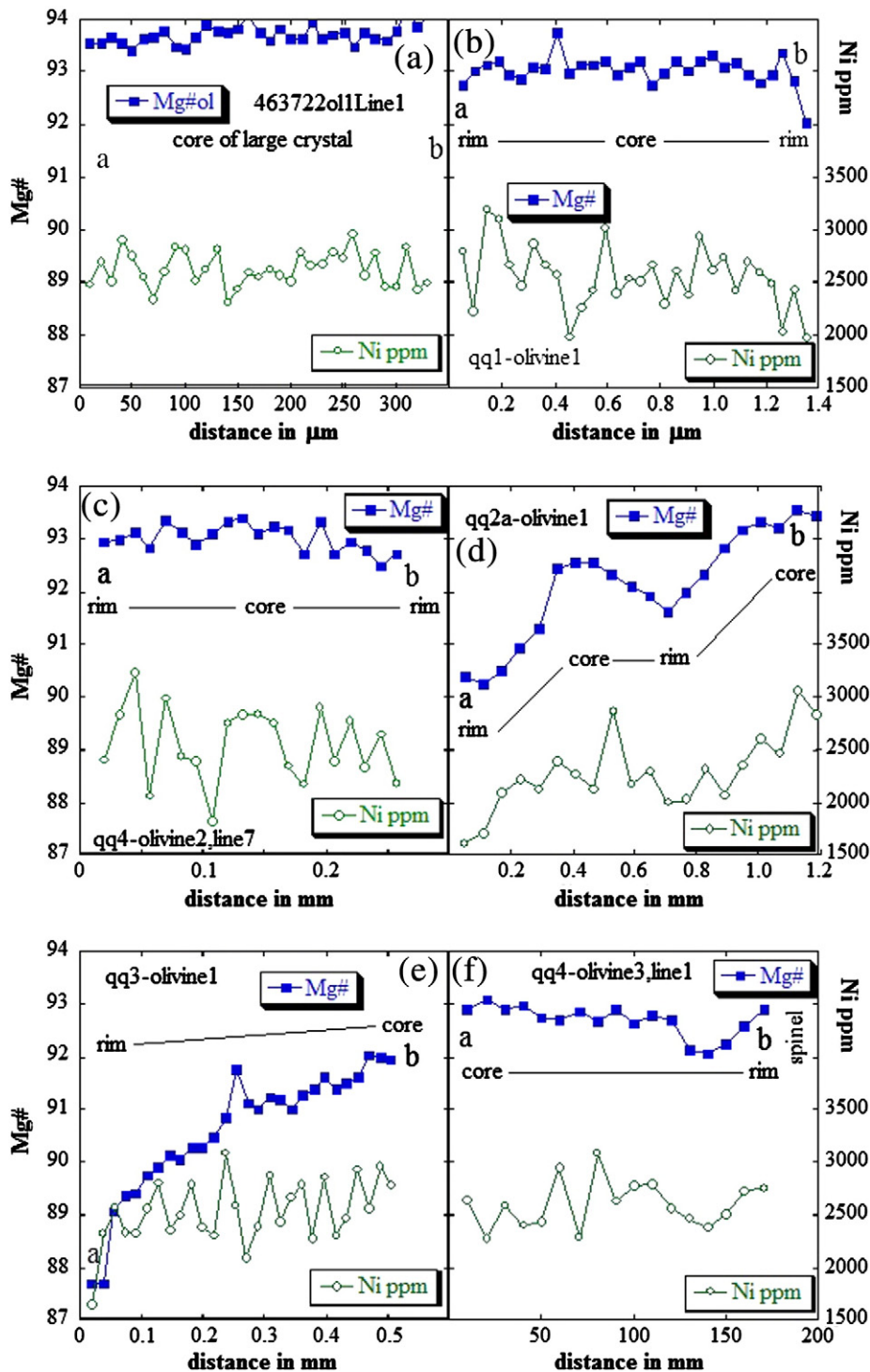


Fig. 5. Representative examples of microprobe traverses across six olivine grains, showing the variation in Mg# and Ni content.

than what is known from olivine in fresh, unaltered mantle xenoliths from Tertiary volcanics and dykes elsewhere in Greenland (Bernstein et al., 1998, 2006).

Some Qeqertaa xenoliths have olivine crystals, such as samples #qq1 and #qq4 (Fig. 5b and c), that show similarly consistent Mg# and Ni concentrations over more than 1 mm traverse and with only a modest zoning with small decreases in Mg# over the outer 0.1 mm of the crystal. These crystals have only weakly altered olivine rims (#qq1, Fig. 5b) or no detectable alteration (#qq4-olivine2, Fig. 5c). Other samples contain olivine grains, which show more pronounced zoning, such as #qq2a-olivine1 and #qq3-olivine1 (Fig. 5d and e), with core

compositions of 93.4 and 92.0, respectively, and rim compositions of 90.3 and 87.7. Ni varies from an average value of about 2500 ppm in the high Mg# region, decreasing to 2000 and then to 1600 ppm at the grain edges. These two olivine crystals are also typical of the more altered versions of olivine, with thick 0.2–0.3 mm alteration rims marked by brown coloration (Fig. 3a). The color seems to stem from minute oxide inclusions, typically less than 1 μm , in the olivine, mainly Fe-oxide, as judged from microprobe data.

One olivine crystal was analyzed with a traverse (Fig. 5f) that runs from crystal core to the edge against a spinel grain (Fig. 7a). The olivine crystal is homogeneous apart from one fracture, which coincides

with a small excursion from a steady level at around Mg# 92.9 to 92.2, accompanied by a small decrease in Ni. The olivine grain terminates at a thin veneer (20 μm wide) of mica that surrounds the spinel grain (Fig. 7a), and the olivine attains its high Mg# and Ni content approaching this contact (Fig. 5f).

4.2. Spinel chemistry

As discussed above, irregular spinel grains or aggregates of magnetite and chromian magnetite are found along cracks and veins in the olivine xenoliths. Spinel textures and occurrence suggest that these irregular grains and aggregates are of secondary origin. Spinel grains with similar texture and composition are also ubiquitous in the matrix and will not be discussed further.

Spinel of likely primary origin is found in portions of the xenoliths, where alteration has been less intense. Some spinel grains interpreted as relic primary spinel are present in the centre of irregular masses or aggregates of iron oxide grains. On the basis of microscopy and backscatter electronic images, it is apparent that two basic types of relic, primary spinel grains occur: 1) some (rare) with recognizable primary grain boundaries, only narrow alteration rims and a less modified core, and 2) more intensely altered grains, with obscured primary grain boundaries, often with overgrowths of chromian magnetite.

The best preserved spinel grains are found as two small (0.1–0.3 mm) slightly translucent grains completely enclosed in a large (12 mm) olivine grain (Fig. 6a). The compositional variation of the core of this olivine grain is presented in Fig. 5a. The two spinel grains are compositionally similar with Cr#, calculated as $\text{Cr}\# = (100 \times \text{Cr}/(\text{Cr} + \text{Al}))$, in the spinel cores of 60.0 ± 0.5 , increasing to a maximum of about 62 at grain edges (Fig. 6b). Mg# and Al#, calculated as $\text{Al}\# = (100 \times \text{Al}/(\text{Fe}^{3+} + \text{Al} + \text{Cr}))$, also show restricted ranges at around 56 and 39, respectively, decreasing slightly at grain edges. $\text{Fe}^{3+}\#$ is very low, mostly between 1 and 2, and increasing slightly to 3–4 at grain edges. ZnO shows slight variation around 0.5 wt.%, while both NiO and TiO_2 is at or below detection limit (Fig. 6d). As examples of the relatively well-preserved spinels of type 1), but with pronounced alteration, Figs. 7a and 8a show two spinel grains in the 100 μm size range. Texturally the two grains are similar, with a translucent core, and a pitted and opaque rim. Spinel grain #qq4b-sp1 (Fig. 7a) is rounded and anhedral, typical for spinel grains in xenoliths of cratonic mantle peridotite, while grain #qq3-sp1 (Fig. 8a) is subhedral. Fine-grained mica aggregates separate the spinel from hosting olivine grains. Chemically, the two spinel grains share some characteristics with relatively constant levels of Cr#, Mg#, $\text{Fe}^{3+}\#$, and Al# in the core, that change markedly at the grain edges towards elevated Cr# and $\text{Fe}^{3+}\#$ and lower Mg# and Al#. This zoning is also pronounced for ZnO, which varies from about 1 wt.% in the centre of the spinel grains to 3 wt.% towards the rim for #qq4-sp1 (Fig. 7d). For spinel #qq3-sp1, the variation and absolute concentrations in ZnO is less extreme with about 0.4–0.7 wt.% (Fig. 8d). For titanium and nickel, core concentrations are ~ 0.1 wt.% increasing to 0.5 wt.% (TiO_2) and ~ 0.3 wt.% (NiO) at the crystal rim (Fig. 7d). Spinel #qq3-sp1 again shows less variation, with 0.2–0.3 wt.% TiO_2 and ≤ 0.1 wt.% NiO (Fig. 8d). MnO follows the pattern of ZnO at similar concentration levels (not shown) for all analyzed spinel grains.

As an example of spinels of type 2), which are more altered and anhedral, Fig. 9 illustrates one grain from sample #qq4, with a short analytical traverse from grain boundary to some way into the core. As for the type 1 spinels in Figs. 7 and 8, a mosaic of mica crystals completely surrounds this spinel, separating it from the host olivine. In this case the mica zone is 50–100 μm wide. The spinel is opaque and the backscatter electron image (Fig. 9a) does not reveal significant zoning, although the rounded shape of the primary spinel can be detected inside the ragged rim. In contrast to the type 1 spinel grains, type 2 shows little variation from core to rim, and instead has extreme Cr#, approaching 100. Mg# is low (< 20) and $\text{Fe}^{3+}\#$ high (> 50). Concentrations of minor elements ZnO and TiO_2 are considerably less variable

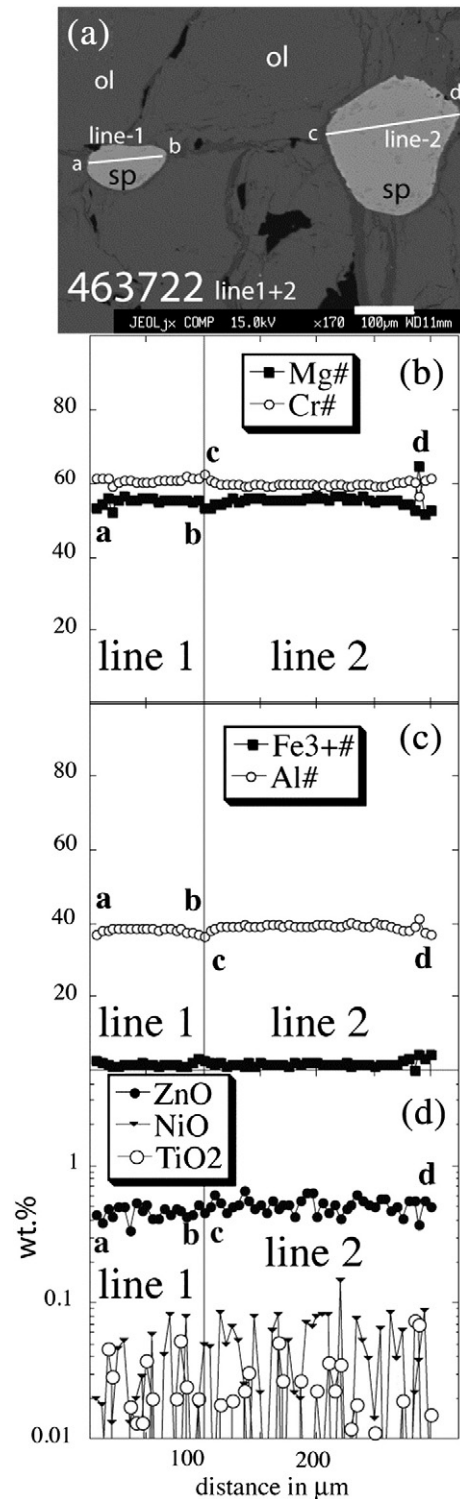


Fig. 6. a) Backscatter electron image of two spinel grains enclosed in a fractured olivine grain from sample #463722. The lines refer to microprobe analyses as presented merged in panels below. b) $\text{Cr}\# = (100 \times \text{Cr}/(\text{Cr} + \text{Al}))$ and $\text{Mg}\# = (100 \times \text{Mg}/(\text{Mg} + \text{Fe}^{2+}))$; d) $\text{Fe}^{3+}\# = (100 \times \text{Fe}^{3+}/(\text{Fe}^{3+} + \text{Al} + \text{Cr}))$ and $\text{Al}\# = (100 \times \text{Al}/(\text{Fe}^{3+} + \text{Al} + \text{Cr}))$. Note the weak zoning only in the outer few tens of micrometers and TiO_2 and NiO around detection limit.

than for type 1 spinel, and typically with values at 0.7–1.0 wt.%, while NiO is low between 0.1 and 0.2 wt.% (Fig. 9d).

From the data presented above it is clear that all spinel grains have undergone variable degrees of chemical modification since the lamprophyre hosting the xenoliths was emplaced. Only a few

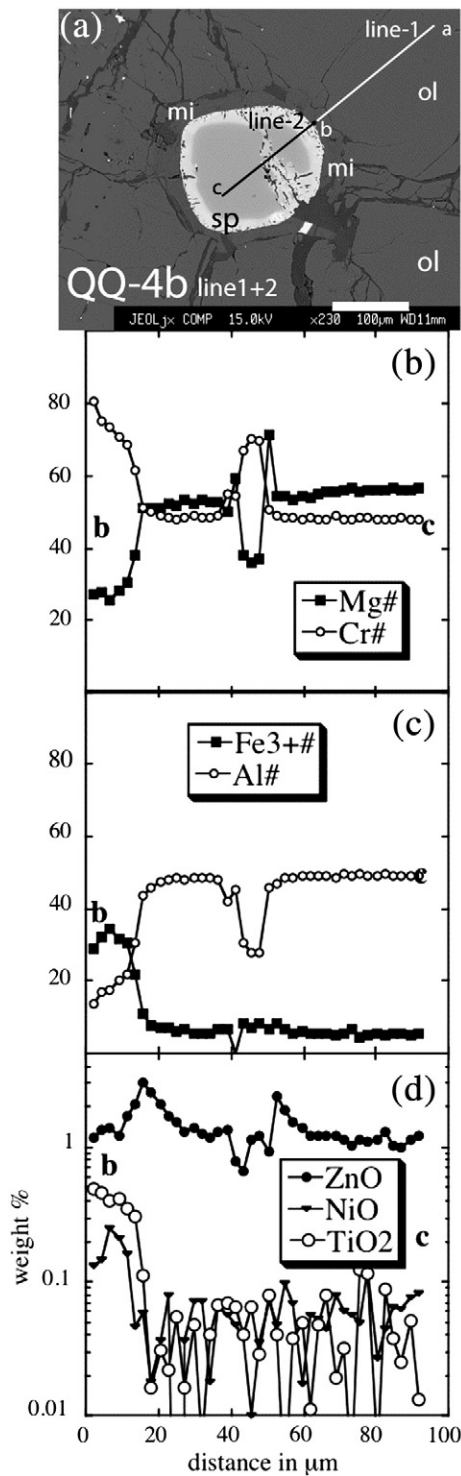


Fig. 7. a) Backscatter electron image of zoned spinel from sample #qq-4b, with lines referring to microprobe analyses as presented in panels below (line-1 is a traverse in olivine and presented in Fig. 5f). b)–d) show chemical variation along the analytical traverse b–c. Note the strong zoning from a relatively homogeneous core to a narrow rim with changes in all depicted chemical parameters. Also note the chemical modification along the crack in the spinel grains, perpendicular to the analytical traverse.

spinel grains have been analyzed with electron microprobe traverses, so it is important to use a chemical parameter that can distinguish between highly altered spinel cores and the less altered cores that potentially retain their primary Cr#. One such parameter is $\text{Fe}^{3+\#}$, which varies from 1.3 to 98.0 in Qeqertaa samples. This is in marked contrast to unaltered and unzoned spinel in mantle xenoliths in Tertiary lavas

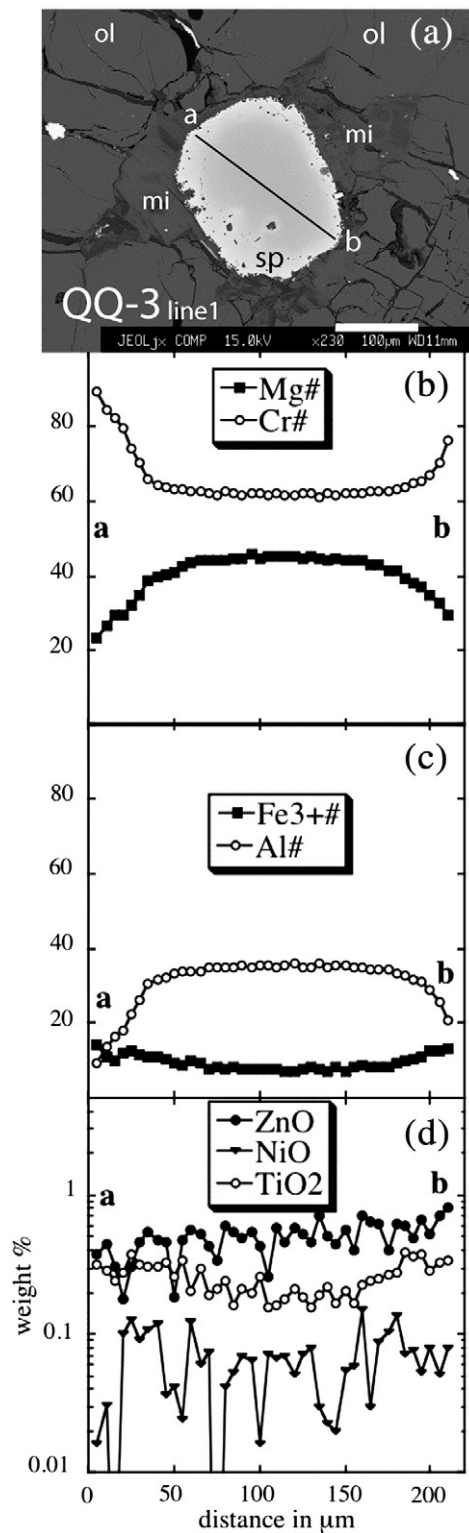


Fig. 8. a) Backscatter electron image of zoned spinel from sample qq-3, with line a–b referring to microprobe analyses as presented in panels below. b)–d) show chemical variation along the analytical traverse b–c (see caption to Fig. 6 for chemical parameters). The data reveals strong zoning from a relatively homogeneous core to a narrow rim with changes in all major element parameters. For the minor elements, Zn, Ni and Ti, there is little variation from core to rim (d).

and dykes in West and East Greenland, which all have $\text{Fe}^{3+\#} < 10$ in spinels that span a Cr# range of 25–95 (Fig. 10). By contrast, Table 1 in the online supplementary material lists all spinel data from Qeqertaa that have $\text{Fe}^{3+\#} < 10$; only 20 samples have such low values.

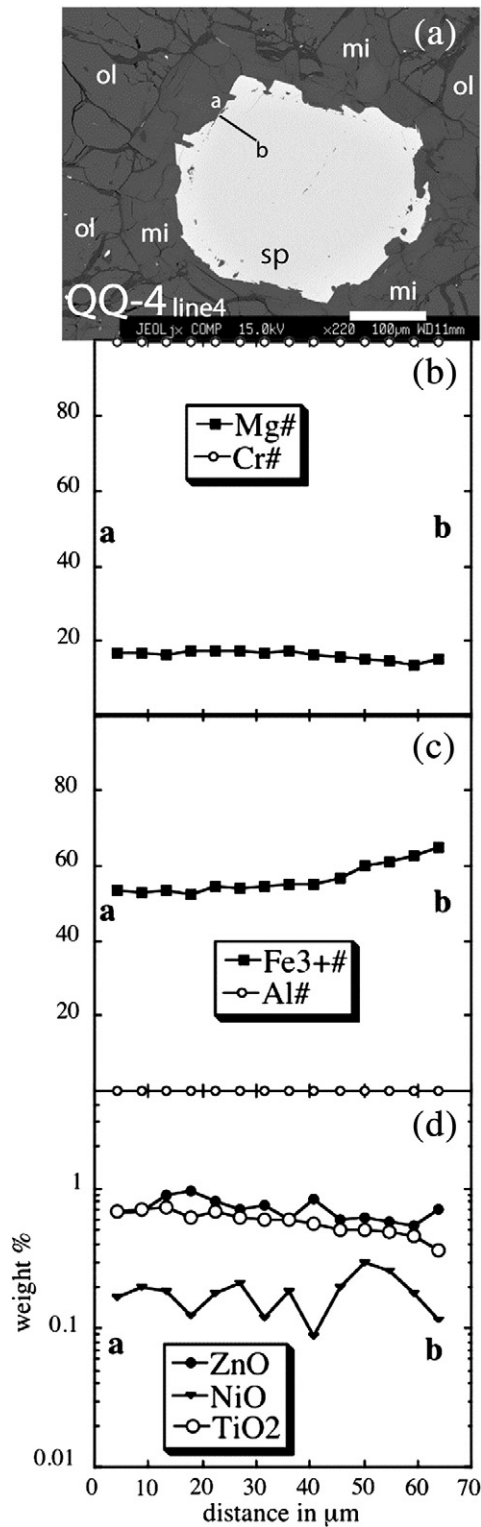


Fig. 9. a) Backscatter electron image of zoned spinel from sample qq-4b, with line a-b referring to microprobe analyses as presented in panels below. b)–d) show chemical variation along analytical traverse a–b (see caption to Fig. 6 for chemical parameters). There is relatively little variation along the traverse, compared to the less altered spinel grains in Figs. 6–8. Note that Cr# is at 100 in b) and Al# is at 0 in c).

Fig. 11 illustrates the compositions of Qeqertaa spinel with $Fe^{3+}\# < 10$. The markedly lower Mg# at a given Cr#, compared to the xenolith suites of Ubekendt Ejland and Wiedemann Fjord, is an indication of lower temperature Fe–Mg exchange with olivine and other silicates in the Qeqertaa spinels. The Qeqertaa samples yield olivine–spinel

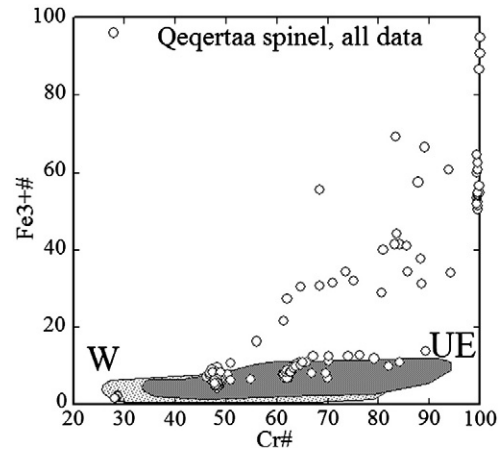


Fig. 10. Chemical variation in terms of Cr# and $Fe^{3+}\#$ comparing all spinel analyses from Qeqertaa xenolith suite with compositions of spinel in mantle xenoliths from Ubekendt Ejland (UE – dark grey field), West Greenland and Wiedemann Fjord (W – light colored field), East Greenland (data from Bernstein et al., 1998, 2006 and unpublished data). Qeqertaa spinel data lying in one of the fields with $Fe^{3+}\#$ less than 10 may have retained their primary Cr#, while those lying outside have been substantially modified during metamorphism.

Fe–Mg exchange temperatures of 400–600 °C (Ballhaus et al., 1991; Sack and Ghiorsio, 1991), which is substantially lower than Ubekendt Ejland (833–960 °C; Bernstein et al., 2006) and Wiedemann Fjord (650–995 °C; Bernstein et al., 1998).

4.3. Orthopyroxene chemistry

The three orthopyroxene grains from three individual xenoliths show a restricted variation, with Mg# spanning 92.7–93.7, and with Cr_2O_3 and Al_2O_3 levels at 0.41–0.52 wt.% and 0.79–0.85 wt.%, respectively (Table 1, online supplementary material). CaO is ca. 1.1 wt.% for two samples, while the remaining sample has only 0.3 wt.% CaO. The three dunite xenoliths that contain orthopyroxene have no garnet, but the high Cr# (26–30) of all three orthopyroxene grains suggests that they have equilibrated with garnet, as orthopyroxene from garnet-free peridotite xenoliths have significantly lower Cr#, mostly less than 20 (Fig. 12). An important note here is that the distinction between orthopyroxene from garnet-bearing and garnet-free peridotite disappears for orthopyroxene with extremely low contents of

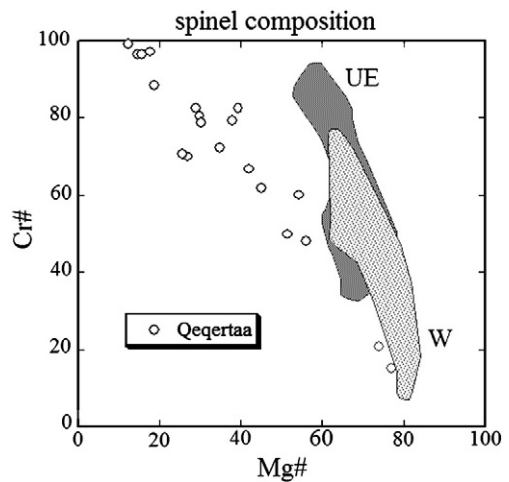


Fig. 11. Spinel from Qeqertaa xenoliths, with the most altered compositions removed (see text and Fig. 10) in terms of Cr# versus Mg#, compared to spinel from Ubekendt Ejland (UE) and Wiedemann Fjord (W) suites. Qeqertaa xenoliths almost span the entire range in Cr#, but have substantially lower Mg#, which is a reflection of lower equilibration temperatures compared to the Ubekendt and Weidemann suites.

Al_2O_3 (<0.2 wt.%), that have variable Cr#, from 4 to 96 (Fig. 12). This is possibly an artefact of poor analytical accuracy or extreme Al depletion during mantle melting and melt extraction in spinel stability field (Bernstein et al., 2007; Stachel et al., 1998). However, the distinction appears robust for orthopyroxene with Al_2O_3 exceeding 0.2 wt.%.

Because of the lack of coexisting phases, such as garnet or clinopyroxene, it is not possible to calculate equilibrium temperatures for the garnet-bearing assemblages, and it is indeed questionable if such calculations would be meaningful, given that the xenoliths were subjected to amphibolite facies metamorphism after emplacement of the Qeqertaa dyke.

5. Discussion

5.1. Metamorphic overprinting

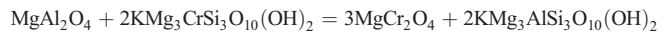
The strongly zoned nature of olivine and chrome spinel from the xenoliths of Qeqertaa is a typical aspect of prograde metamorphism of altered peridotite (e.g. Evans and Frost, 1975; Nozaka, 2003; Trommsdorff et al., 1998; Vance and Dungan, 1977). The Qeqertaa olivines with brown, inclusion-rich grain margins show textural similarity to hydrothermally altered olivine xenocrysts and xenoliths from Venetia kimberlites, South Africa (Stripp et al., 2006), where thin talc rims form on serpentinized olivine grains. In a study of olivine compositional variation in Chugoku peridotite (Japan), which has been subjected to steep local metamorphic gradients, Nozaka (2003) demonstrates how primary olivine with Mg# around 91 can attain both higher (to 97.6) and lower (to 86) Mg# during prograde reactions. The assemblage at Qeqertaa of coexisting olivine, tremolite and talc is analogous to metamorphic zone 3 of Nozaka (2003, and references therein), where essentially all olivine is metamorphic. The metamorphic olivine in Chugoku peridotites forms overgrowths, along distinct grain boundaries and 'healed' cracks or veins, where olivine replaces serpentine. Magnetite-free serpentine is thought to be the precursor of high-Mg# olivine, while low-Mg# olivine is thought to crystallize from magnetite-bearing serpentine. The olivine in Qeqertaa xenoliths always shows normal

zoning with low-Mg# zones crowded with minute Fe-oxide inclusions. These low-Mg# rims are thus likely to represent recrystallized, partly serpentinized olivine with Fe-oxide grains remaining from the hydrothermally reacted olivine.

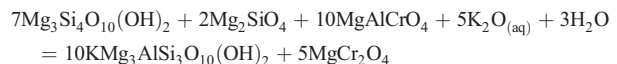
In Qeqertaa xenoliths, all olivine grains show some reaction along grain boundaries, evident from the presence of either hydrous phases, such as talc, or fine-grained Fe-oxide inclusions. However, many olivine grain centres are colorless, transparent and inclusion-free down to the resolution of the electron microprobe. These olivine cores coincide with maximum Mg# in the individual olivine and suggest that the cores represent primary olivine that escaped extensive serpentinization. Likewise, the typical coarse protogranular texture (Fig. 3) suggests that the Qeqertaa xenoliths are not entirely recrystallized from serpentine or talc during prograde metamorphism, as such recrystallization commonly forms equigranular olivine aggregates or highly elongate olivine resembling spinifex texture (e.g. Trommsdorff et al., 1998). Another piece of evidence for the colorless olivine to have escaped the initial serpentinization is the presence of inclusions of pale, inclusion-free phlogopite crystals that are in strong contrast to the dark-brown, inclusion-rich mica phenocrysts or xenocrysts in the groundmass.

The relatively robust nature of chromite makes these a potential powerful recorder of alteration processes (e.g. Barnes, 2000; Evans and Frost, 1975; Kimball, 1990). The types of chemical zoning depicted in Figs. 6–9 can be explained in terms of hydrothermal alteration followed by prograde metamorphism from primary chromite with slightly altered crystal rims to magnetite rimmed spinel grains with equilibrated cores. The high ZnO (mostly at 0.4–3.0 wt.%) present in all spinel grains with electron probe traverses, show that even spinel cores have been modified by metamorphic reactions, because primary spinels have ZnO at the 0.1 wt.% level, at least in komatiite flows (Barnes, 2000). The exception is the spinel portrayed in Fig. 6a, which perhaps escaped strong modification. Certainly, some spinel has been altered to magnetite, which is found in cracks and veins, as well as along olivine grain boundaries (Fig. 3). This suggests at least some degree of early partial serpentinization and later recrystallization of olivine, which would then leave magnetite interstitially between olivine crystals as seen in Fig. 3.

The spinel grains in 463722 and #qq-4b (Figs. 6 and 7) are morphologically the least altered spinel grains of those analyzed. The lack of a thick, euhedral Fe-spinel jacket suggests that these grains have remained relatively undisturbed during metamorphism. While the zoning in the two spinel grains in 463722 is very modest, #qq-4b shows a more pronounced decrease of magnesium and aluminium towards the rim and around the transecting crack, which is typical for chromite equilibrating with olivine, talc, or ferroan magnesite (for Mg) and chlorite (for Al) (Barnes, 2000). In the case of the Qeqertaa xenoliths, the samples lack chlorite. However, Cr–Al exchange between spinel and mica, as in the following simplified reaction, would decrease the Al content of spinel:



Instead or in addition, metamorphic reactions forming mica from talc + olivine + aluminous spinel + fluid, as in the following simplified example, could also explain the high Cr# in remaining Qeqertaa spinels:



The occurrence of one or both of these reactions is consistent with the phlogopite-rich composition of the mica that coats the spinel in for example Fig. 7a) at the end of line-1 (see supplementary data Table 1).

Following Barnes' (2000) study, serpentinization of dunite xenoliths and olivine in the lamprophyre matrix results in decomposition of olivine and release of Zn. Chromite absorbs Zn, resulting in a steep concentration profile from high ZnO at altered chromite rims to very

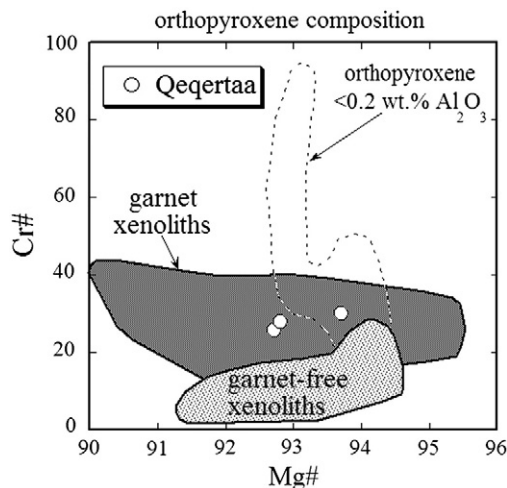


Fig. 12. Composition of orthopyroxene (in the only three samples found to contain orthopyroxene), in terms of Cr# and Mg#. Also shown are compositional fields for orthopyroxene from Greenlandic garnet-bearing xenoliths (Sarfartoq–Maniitsoq region; Garrit, 2000) and from garnet-free, spinel-bearing xenoliths from Ubekendt Eiland, Wiedemann Fjord and Sarfartoq–Maniitsoq (Bernstein et al., 1998, 2006; Garrit, 2000, respectively). Only orthopyroxene with $\text{Al}_2\text{O}_3 > 0.2$ wt.% is included in the bodies of data for garnet-free xenoliths. Some orthopyroxene with $\text{Al}_2\text{O}_3 < 0.2$ wt.% show a much greater variation in Cr# (stippled field), which is possibly an artifact of poor analytical accuracy close to the detection limit.

low concentration (<0.1 wt.%) at unaltered chromite cores. Prograde metamorphism to amphibolite facies subsequently redistributes Zn in the chromite grains and tends to homogenize concentration differences, which in turn also results in elevated Zn in grains that have retained their primary Cr# (Barnes, 2000).

In a more extreme case, such as in Fig. 9 (#qq4, line4) aluminium is completely lost, along with most of the magnesium. The overgrowth of Fe-rich spinel exhibits crystal faces, but still contains appreciable amounts of Cr. In fact, only a few of the analyzed chrome spinel grains have pure magnetite rims. In a plot of all spinel analyses in terms of their trivalent cations (Fig. 13) these highly altered grains (as in Fig. 9), and altered spinel rims (Figs. 7–8) plot along the Cr–Fe³⁺ join, clustering at Cr₃₀Fe³⁺₇₀–Cr₅₀Fe³⁺₅₀ and connecting to the main body of spinel data along the Al–Cr join at low (generally <10%) Fe³⁺. These intermediate spinel compositions suggest extensive solid solution between the spinel end-member components (Fe, Mg)Cr₂O₄, (Fe, Mg)Al₂O₄ and (Fe, Mg)Fe₂O₄ and thus equilibration temperatures above 600 °C according to Sack and Ghiorso (1991). At temperatures at or below 550 °C the solid solution stability field is significantly reduced by miscibility gaps, which expand with decreasing temperature, resulting in formation of coexisting chromite and Cr-poor magnetite (see also Barnes, 2000). The presence of intermediate compositions in the Qeqertaa xenoliths suggests crystallization above the solvus.

Fig. 10 shows that most spinel analyses have high Fe³⁺# (>10) reflecting the effects of hydrothermal alteration and/or amphibolite facies metamorphism. However, even spinel with Fe³⁺# <10 have lost their primary Mg# as seen in Fig. 11. The least altered Qeqertaa xenoliths plot along the metamorphic trend identified by Evans and Frost (1975). As in most alpine peridotite massifs, Fe–Mg exchange between spinel and olivine has reduced spinel Mg#.

Primary spinel Cr# can in some cases be preserved in metamorphosed peridotites. The range of Cr# in Qeqertaa spinels overlaps with that of Ubekendt Ejland and Wiedemann Fjord xenolith suites, raising the possibility that some crystals retain primary Cr#s. However, Qeqertaa xenolith spinels plot along the metamorphic Cr# versus Mg# trend of Evans and Frost (1975) for spinels in chlorite-bearing metaperidotites. Very high

Cr# and low Mg# in metamorphic spinels were also observed by Barnes and Roeder (2001), further suggesting that Qeqertaa spinel Cr#s may have been modified by metamorphic reactions, perhaps to some degree even for spinels with low Fe³⁺#.

In summary, the combined evidence from olivine and spinel points to a history of partial replacement of olivine by serpentine during hydrothermal alteration, followed by prograde metamorphism to amphibolite facies, as suggested by the presence of recrystallized olivine rims, the character of zoned chrome spinel, and olivine–spinel Fe–Mg thermometry.

5.2. Primary olivine compositions

Considering olivine cores only, the Qeqertaa xenoliths have an average Mg# of 92.6 with a median Mg# of 92.8. Given the considerable zoning, these values are probably minimum estimates of the average and median, values of primary Mg#, because (a) some apparent olivine cores may be from olivine in which the plane of the thin section is parallel to and close to one edge of the crystal, and therefore have broad areas of low-Mg#, and (b) even some of the larger, clear grains may be neoblasts, crystallized from completely serpentinized primary olivine. In any case, olivines from Qeqertaa xenoliths have highly refractory compositions that are typical for dunite and harzburgite xenolith suites from the lithospheric mantle beneath Archaean cratons (e.g. Bernstein et al., 1998, 2006, 2007; Boyd, 1989; Boyd et al., 1997; Canil, 2004; Lee and Rudnick, 1999; Menzies, 1990; Pearson et al., 2003; Wittig et al., 2008).

The large range in olivine Ni concentrations (1328 ppm to 4008 ppm) portrayed in Fig. 4 and in detail for a subset of individual olivine crystals in Fig. 5, is not easily explained. Some of the range may reflect the redistribution of Ni during partial serpentinization and subsequent prograde metamorphism as discussed above. One likely example is shown in Fig. 5d, in which the recrystallized olivine rim shows substantially lower Mg# and variable but overall decreasing Ni content compared to olivine core. However, even for colorless, inclusion-free olivine grains or olivine cores, there appears to be considerable variation in Ni content. Our microprobe traverses of seemingly unaltered olivine cores with near-constant Mg# reveal Ni variation spanning 2000–3000 ppm over few hundred microns (Fig. 5b, c and f), although one grain (Fig. 5a) shows a much tighter variation in Ni with values between 2400 and 2900 ppm. One potential explanation for such variation could be that all olivine is of metamorphic origin, which in turn implies that the low-temperature hydrothermal alteration altered the entire peridotite mineral assemblage prior to the prograde metamorphism. We find this to be implausible not only on textural grounds as described in Section 5.1 but also because rare, large, pale mica crystals in the dunite xenoliths are free of the magnetite inclusions that dominate the altered mica crystals in the groundmass. We find it unlikely that a phlogopite crystal would maintain its textural integrity if it were engulfed in completely serpentinized dunite.

During our microprobe work on the olivine, we have not detected any inhomogeneity by back-scatter imagery and the origin of the Ni variation is therefore uncertain. While it could stem from minute sulphide inclusions, we also note that the majority of the analytical values are within the normal range for olivine from olivine-rich, residual mantle peridotites (2000–3500 ppm; e.g., Bodinier and Godard, 2003). We note that the range in Ni for the Qeqertaa xenolithic olivine is similar to that observed for other xenolith suites in the North Atlantic craton which may suggest that this is a common feature (e.g. Bernstein et al., 1998, 2006; Wittig et al., 2008). One possibility is that early (prior to peridotite entrapment in lamprophyre) melt–rock reaction could be responsible for some of the decrease in Ni content of olivine, such as is observed in dunite replacing harzburgite in the Bay of Island ophiolite (Suhr et al., 2003). However, we do not currently have trace element data to test if melt–rock reactions were significant in this case. Variable Ni concentrations, with very low values in some parts of olivine crystals,

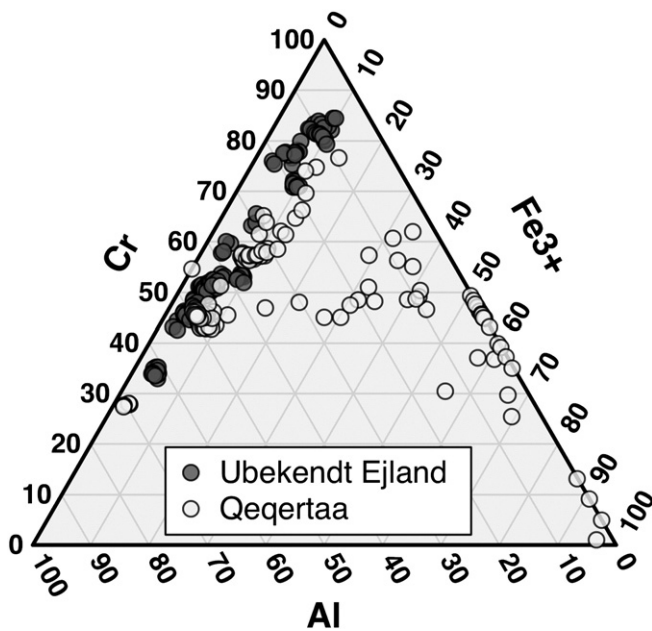


Fig. 13. Spinel compositions from analytical traverses by electron microprobe in five spinel grains from the Qeqertaa xenolith suite, compared with unaltered spinel in mantle xenoliths from Ubekendt Ejland, West Greenland (Bernstein et al., 2006). The three components represent atomic proportions referring to the spinel formula, with Fe³⁺ calculated assuming stoichiometry.

could also be due to the presence of sulfides during peridotite recrystallization in the mantle. This is observed in sulfide-rich dunites from Oman (Negishi et al., *in press*). However, no sulphides have been observed in any of the Qeqertaa xenoliths. Another potential process that might account for the large variability of Ni in olivine is nickel redistribution during early pervasive serpentinization, followed by later prograde recrystallization. We reiterate that the large Ni variation in olivine appears to be a common feature in Greenlandic xenolith suites, regardless of their emplacement age or post-emplacement thermal history. A systematic study of nickel content in olivine for all Greenlandic xenolith suites could address this question.

With respect to the nearly monomineralic composition of the Qeqertaa xenoliths, they are similar to the shallow, garnet-free, spinel dunites from Ubekendt Ejland, and the olivine-rich, orthopyroxene-poor spinel harzburgites from Wiedemann Fjord (average ca. 12 wt.% orthopyroxene). All three suites have similar average olivine compositions of Mg# 92.6–92.8 (Bernstein et al., 1998, 2006, 2007). The growing body of data on cratonic mantle xenoliths from Greenland suggests that such olivine-rich mantle may be more common here than in other cratons, and perhaps is the most abundant lithology in the shallow, cratonic mantle beneath some parts of Greenland. Sample collections from Southwest Greenland (some 300–800 km south of Disko Bay) have peridotite xenolith suites typically ranging from 75 to 100% modal olivine, with compositions averaging Mg# 92.5–92.8 (Bizzarro and Stevenson, 2003; Garrit, 2000; Wittig et al., 2008). In other cratons, such as Kaapvaal, Tanzania, Siberia, and Slave, mantle xenolith suites typically have lower modal olivine and higher orthopyroxene, with ranges of 40–80% olivine and 20–60% orthopyroxene, plus additional spinel, clinopyroxene and garnet (see compilations of e.g. Griffin et al., 2003; Herzberg, 1993; Lee, 2006; Pearson et al., 2003).

It has long been clear that the high Mg# of olivine in cratonic mantle peridotite exceeds that of olivine from Phanerozoic abyssal peridotite, most orogenic peridotite massifs and most peridotite from arcs (Bonatti and Michael, 1989; Boyd, 1989; Boyd and Mertzman, 1987; Menzies, 1990; Nixon and Boyd, 1973) and that this elevated Mg# in olivine and bulk rock compositions likely stems from higher extents of partial melting in the Archaean (Boyd, 1989; Herzberg et al., 2010; Jordan, 1975; O'Hara et al., 1975). The nature of the melting processes has on the other hand been subject to much debate over the last couple of decades, mainly because the orthopyroxene-rich mantle peridotites beneath Kaapvaal and some other cratons, such as Yakutia in Siberia, for many years were considered representative of cratonic mantle. The high proportion of orthopyroxene (often >40 wt.%) in these peridotite xenoliths is considered inconsistent with an origin as residues of melt extraction from primitive upper mantle compositions (e.g. Herzberg, 1993; Kelemen et al., 1998; Kesson and Ringwood, 1989; Walter, 1998).

Following the discovery of depleted orthopyroxene-poor xenoliths from Greenland and some other cratons (Bernstein et al., 1998, 2007; Boyd and Canil, 1997; Larsen, 1982) it has become widely accepted that such high-Mg#, orthopyroxene poor harzburgites and dunites, and olivine + spinel inclusions in diamonds, can be viewed as archetypical cratonic mantle peridotite (e.g. Bernstein et al., 2007; Pearson and Wittig, 2008) formed by melt extraction of 37–45% (e.g. Herzberg, 2004). The modal composition of orthopyroxene-poor harzburgite and dunite cratonic xenoliths and their high Mg# suggest that they are residues of polybaric decompression melting starting at 4 to 6 GPa and extending to less than 3 GPa (Bernstein et al., 1998, 2006; Herzberg, 2004; Kelemen et al., 1998; Walter, 2003). Depending on the nature of melting and melt extraction (“equilibrium porous flow” versus “fractional melting”), this may be consistent with the observation that the trace element composition of SCLM xenoliths from several cratons suggests melting at a shallow depth (<3 GPa; e.g. Canil, 2004; Wittig et al., 2008). Alternatively, high Mg# and other indications of extreme melt depletion could be the cumulative result of multiple stages, each with a moderate degree of melt extraction. The uniform olivine Mg# of 92.6–92.8 of the cratonic high Mg# dunite may have been controlled by the exhaustion

of orthopyroxene during melt extraction, limiting the maximum extent of melt depletion to about 40% in most cases, regardless of the tectonic environment (Bernstein et al., 2007).

Likewise, there is a growing consensus that the orthopyroxene-rich nature of mantle peridotite beneath e.g. Kaapvaal, is a result of silica addition through melt–rock reaction, in which silica-rich melts react with a high-Mg# dunite protolith, perhaps in the hanging wall of a subduction zone (Gibson et al., 2008; Griffin et al., 2009; Kelemen et al., 1998; Kesson and Ringwood, 1989; Lee, 2006; Lee et al., 2011; Pearson and Wittig, 2008; Rudnick et al., 1994). Indeed, the data and interpretations of Hanghøj et al. (2001) and Bernstein et al. (2007) suggest that Al as well as Si has been added to dunite protoliths in most cratonic harzburgites, and that some cratonic lherzolites are also refertilized dunites, modified by addition of Ca, Fe, Al, Si, and probably many other elements.

Pressure and temperature at the time of xenolith entrainment can be calculated for many garnet-bearing peridotite xenoliths. Pressures indicate depths of equilibration in the order of 2.5–7 GPa or about 75–220 km depth (e.g. Lee, 2006). Disregarding xenoliths with clear signs of metasomatic overprinting by a basaltic/basanitic or carbonatitic melt (i.e. presence of abundant diopside, amphibole, mica, carbonate, rutile, etc.), there is a surprisingly constant and high Mg# of olivine in cratonic mantle, from 91.5–94.0 for most cratons, with averages spanning 92.0 to 93.0 (e.g. Gaul et al., 2000; Griffin et al., 2003; Pearson and Wittig, 2008), which do not correlate with depth of equilibration. These values are similar to depleted, garnet-free spinel peridotite xenoliths from the cratons, which also have average olivine Mg# of 92.5–92.8 (Bernstein et al., 2007).

As noted above, the bulk composition of most garnet-bearing cratonic mantle xenoliths reflects low pressure melting in the absence of garnet (e.g. Canil and Wei, 1992; Kelemen et al., 1998; Stachel et al., 1998) despite their deep residence at the time of entrainment. The trend of bulk compositions, with correlated Ca and heavy rare earth element concentrations, demonstrate that few if any cratonic peridotites contain residual garnet. Instead, most garnets in the cratonic upper mantle must be metamorphic in origin (Kelemen et al., 1998). This interpretation requires that low-pressure peridotite residues of decompression melting have been transported to depth at some later stage, possibly during collision of tectonic plates leading to stacking of the depleted and hence buoyant dunitic restite (e.g. Gray and Pysklywec, 2010; Helmstaedt and Schulze, 1989) or via ascent and accumulation of buoyant, Fe-poor peridotite diapirs (e.g., Oxburgh and Paramentier, 1977; Oxburgh et al., 1978).

In this light, the presence of garnet-bearing dunite with average olivine Mg# of 92.6 in the Qeqertaa suite, considered together with the garnet-free Ubekendt and Weidemann xenolith suites, shows that by Palaeoproterozoic time, the mantle beneath this part of the North Atlantic craton included regionally extensive high Mg# dunite extending from depths within the spinel peridotite stability field (Bernstein et al., 2006), deep into the garnet peridotite stability field, and indeed into the diamond stability field as documented by the presence of diamonds in the Qeqertaa dyke (Marmo et al., 2012). Along typical cratonic conductive geotherms (surface heat flow of 40–50 mW/m²), this results in a vertical distribution of high-Mg# dunite over 150 km of the lithospheric mantle.

6. Conclusions

We have shown that yet another SCLM xenolith suite from Greenland records consistently high Mg# in olivine. The Qeqertaa xenoliths have average olivine Mg# of 92.6 and a median value of 92.8, which appears to be the dominating composition for SCLM in the North Atlantic craton.

The presence of garnet in five xenoliths, suggests an equilibration pressure greater than 2.5 GPa (>75 km depth). The presence of diamonds in the Qeqertaa dyke demonstrates that the SCLM in this

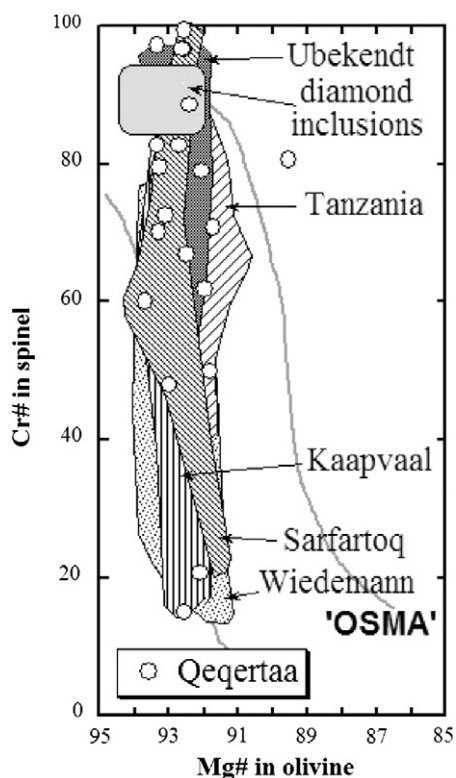


Fig. 14. Cr# in spinel versus Mg# in olivine from different cratonic xenolith suites. Qeqertaa xenoliths plot on top of this array and their Cr# covers the entire range. Diamond inclusions on the other hand are restricted to Cr# around 90. The background data are from the literature as follows: Ubekendt (Bernstein et al., 2006), diamond inclusions (Stachel et al., 1998), Tanzania (Rudnick et al., 1994), Kaapvaal (Herzberg, 2004), Sarfartoq (Bizzarro and Stevenson, 2003; Garrit, 2000), Wiedemann (Bernstein et al., 1998) and OSMA (Arai, 1994).

region must have been more than 150 km thick prior to the Palaeoproterozoic transport of the xenoliths into the crust.

After emplacement in the crust, Qeqertaa xenoliths likely equilibrated at temperatures slightly above 600 °C, as reflected in their spinel compositions, during amphibolite facies metamorphism in the crust. The Cr# versus Mg# trend of spinel from Qeqertaa is different than for xenoliths from Ubekendt Eiland and Wiedemann Fjord (Bernstein et al., 1998, 2006), although they probably shared a similar origin in highly depleted, residual dunites.

Unlike spinel Mg#'s, which are typically modified during metamorphism, spinel Cr#'s can in some cases preserve primary, residual compositions. Values of $Fe^{3+}/\# < 10$ in some Qeqertaa spinels suggest that primary Cr# may have been preserved in a few cases. However, the Qeqertaa xenolith spinels plot along the metamorphic Cr# versus Mg# trend for chlorite-bearing peridotites identified by Evans and Frost (1975). Our samples do not contain chlorite, but they do contain metamorphic mica separating spinels from host olivine crystals. This suggests that even spinel Cr# can be modified by open behavior during amphibolite facies metamorphism. Thus, care must be taken when interpreting the geological formation environment of metamorphic mantle rocks, in terms of their spinel composition.

The surprisingly monotonous lithology in the 100% dunite Qeqertaa xenolith suite further supports the hypothesis that much of the cratonic mantle is composed of low pressure residues of high degrees of decompression melting, limited by the exhaustion of orthopyroxene (Bernstein et al., 2007). The Qeqertaa data are similar to xenolith data from other areas of the North Atlantic craton, as well as some other cratons as seen in Fig. 14, which supports the hypothesis that olivine-rich dunites and harzburgites with Mg# around 92.8 represent the pristine composition of SCLM, prior to refertilization via melt–rock reaction.

Supplementary data to this article can be found online at <http://dx.doi.org/10.1016/j.lithos.2013.02.011>.

Acknowledgements

We thank Jacques Deleuran, Birgit Leer and Marie Leer Jørgensen for assistance during xenolith sampling and Artisk Station (University of Copenhagen) and its ship R/V Porsild for transportation and other field support. Berit Wenzel and Alfons Berger helped with the electron microprobe. Thanks also to Minik Rosing and NordCEE for supporting the senior author. We thank G. Nelson Eby for editorial handling of the manuscript and Claude Herzberg and one anonymous reviewer for constructive comments on an early version.

References

- Arai, S., 1994. Characterization of spinel peridotites by olivine–spinel compositional relationships: review and interpretation. *Chemical Geology* 113, 191–204.
- Aulbach, S., Stachel, T., Heamann, M., Creaser, R.A., Shirey, S.B., 2011. Formation of cratonic subcontinental lithospheric mantle and complementary komatiite from hybrid plume sources. *Contributions to Mineralogy and Petrology* 161, 947–960.
- Ballhaus, C., Berry, R.F., Green, D.H., 1991. High pressure experimental calibration of the olivine–orthopyroxene–spinel oxygen barometer: implications for the oxidation state of the mantle. *Contributions to Mineralogy and Petrology* 107, 27–40.
- Barnes, S.J., 2000. Chromite in komatiites II. Modification during greenschist to mid-amphibolite facies metamorphism. *Journal of Petrology* 41, 387–409.
- Barnes, S.J., Roeder, P.L., 2001. The range of spinel compositions in terrestrial mafic and ultramafic rocks. *Journal of Petrology* 42, 2279–2302.
- Bernstein, S., Kelemen, P.B., Brooks, C.K., 1998. Depleted spinel harzburgite xenoliths in Tertiary dykes from East Greenland: restites from high degree melting. *Earth and Planetary Science Letters* 154, 221–235.
- Bernstein, S.K., Hanghøj, K., Kelemen, P.B., Brooks, C.K., 2006. Ultra-depleted, shallow cratonic mantle beneath West Greenland: dunitic xenoliths from Ubekendt Eiland. *Contributions to Mineralogy and Petrology* 152, 335–347.
- Bernstein, S., Kelemen, P.B., Hanghøj, K., 2007. Consistent olivine Mg# in cratonic mantle reflects Archean mantle melting to the exhaustion of orthopyroxene. *Geology* 35, 459–462.
- Bizzarro, M., Stevenson, R.K., 2003. Major element composition of the lithospheric mantle under the North Atlantic craton: evidence from peridotite xenoliths of the Sarfartoq area, southwestern Greenland. *Contributions to Mineralogy and Petrology* 146, 223–240.
- Bodinier, J.-L., Godard, M., 2003. Orogenic, ophiolitic and abyssal peridotites. In: Holland, H.D., Turekian, K.K. (Eds.), *Treatise on Geochemistry*, vol. 2. Elsevier.
- Bonatti, E., Michael, P.J., 1989. Mantle peridotites from continental rifts to ocean basins to subduction zones. *Earth and Planetary Science Letters* 91, 297–311.
- Boyd, F.R., 1989. Compositional distinction between oceanic and cratonic lithosphere. *Earth and Planetary Science Letters* 96, 15–26.
- Boyd, F.R., Canil, D., 1997. Peridotite xenoliths from the Slave craton, Northwest Territories. Seventh Annual V. M. Goldschmidt Conference, LPI Contribution No. 921. Lunar and Planetary Institute, Houston.
- Boyd, F.R., Mertzman, S.A., 1987. Composition and structure of the Kaapvaal lithosphere, southern Africa. Magmatic processes. In: Mysen, B.A. (Ed.), *Physicochemical Principles: The Geochemical Society, Special Publication*, 1, pp. 13–24 (University Park, PA).
- Boyd, F.R., Pokhilenko, N.P., Pearson, D.G., Mertzman, S.A., Sobolev, N.V., Finger, L.W., 1997. Composition of the Siberian cratonic mantle: evidence from Udachnaya peridotite xenoliths. *Contributions to Mineralogy and Petrology* 128, 228–246.
- Canil, D., 2004. Mildly incompatible elements in peridotite and the origins of mantle lithosphere. *Lithos* 77, 375–393.
- Canil, D., Wei, K., 1992. Constraints on the origin of mantle-derived low Ca garnets. *Contributions to Mineralogy and Petrology* 109, 421–430.
- Evans, B.W., Frost, B.R., 1975. Chrome–spinel in progressive metamorphism – a preliminary analysis. *Geochimica et Cosmochimica Acta* 39, 959–972.
- Garde, A.A., Steenfelt, A., 1999. Precambrian geology of Nuussuaq and the area north-east of Disko Bugt, West Greenland. *Geology of Greenland Survey Bulletin* 181, 6–40.
- Garrit, D., 2000. The nature of the Archean and Proterozoic lithospheric mantle and lower crust in West Greenland illustrated by the geochemistry and petrography of xenoliths from kimberlites. unpublished ph. d. thesis University of Copenhagen, 289.
- Gaul, O.F., Griffin, W.L., O'Reilly, S.Y., Pearson, N.J., 2000. Mapping olivine composition in the lithospheric mantle. *Earth and Planetary Science Letters* 182, 223–235.
- Gibson, S.A., Malarkey, J., Day, J.A., 2008. Melt depletion and enrichment beneath the western Kaapvaal Craton: evidence from Finsch peridotite xenoliths. *Journal of Petrology* 49, 1817–1852.
- Gray, R., Pysklywec, R.N., 2010. Geodynamic models of Archean continental collision and formation of mantle lithosphere keels. *Geophysical Research Letters* 37 (L19301), 1–5.
- Griffin, W.L., O'Reilly, S.Y., Abe, N., Aulbach, S., 2003. The origin and evolution of Archean lithospheric mantle. *Precambrian Research* 127, 19–41.
- Griffin, W.L., O'Reilly, S.Y., Afonso, J.C., 2009. The composition and evolution of lithospheric mantle: a re-evaluation and its tectonic implications. *Journal of Petrology* 50, 1185–1204.

- Hanghøj, K., Kelemen, P., Bernstein, S., Blusztajn, J., Frei, R., 2001. Osmium isotopes in the Wiedemann Fjord mantle xenoliths: a unique record of cratonic mantle formation by melt depletion in the Archaean. *Geochemistry, Geophysics, Geosystems* 2 (2000GC000085).
- Helmstaedt, H.H., Schulze, D.J., 1989. Southern African kimberlites and their mantle sample: implications for Archaean tectonics and lithosphere evolution. *Geological Society of America Special Publications* 14, 358–368.
- Herzberg, C.T., 1993. Lithosphere peridotites of the Kaapvaal Craton. *Earth and Planetary Science Letters* 120, 13–29.
- Herzberg, C., 2004. Geodynamic information in peridotite petrology. *Journal of Petrology* 45, 2507–2530.
- Herzberg, C., Condie, K., Korenaga, J., 2010. Thermal history of the earth and its petrological expression. *Earth and Planetary Science Letters* 292, 79–88.
- Jordan, T.H., 1975. The continental tectosphere. *Reviews of Geophysics* 13, 1–12.
- Kelemen, P.B., Hart, S.R., Bernstein, S., 1998. Silica enrichment in the continental lithosphere via melt/rock reaction. *Earth and Planetary Science Letters* 164, 387–406.
- Kesson, S.E., Ringwood, A.E., 1989. Slab-mantle interactions 1. Sheared and refertilized garnet peridotite xenoliths – samples of Wadati–Benioff zones? *Chemical Geology* 78, 83–96.
- Kimball, K.L., 1990. Effects of hydrothermal alteration of the compositions of chromian spinels. *Contributions to Mineralogy and Petrology* 105, 337–346.
- Larsen, J.G., 1982. Mantle-derived dunite and lherzolite nodules from Ubekendt Eiland, west Greenland Tertiary province. *Mineralogical Magazine* 46, 329–336.
- Larsen, L.M., Rex, D.C., 1992. A review of the 2500 Ma span of alkaline-ultramafic, potassic and carbonatitic magmatism in West Greenland. *Lithos* 28, 367–402.
- Lee, C.-T., 2006. Geochemical/petrologic constraints on the origin of cratonic mantle. Archaean geodynamics and environments. In: Benn, K., Mareschal, J.-C., Condie, K.C. (Eds.), *Geophysical Monograph. American Geophysical Union*, pp. 89–114.
- Lee, C.-T., Rudnick, R.L., 1999. Compositionally stratified cratonic lithosphere: petrology and geochemistry of peridotite xenoliths from the Labait Volcano, Tanzania. *Proceedings of the 7th International Kimberlite conference Red Roof Design, Cape Town*, pp. 503–521.
- Lee, C.T.A., Luffi, P., Chin, E.J., 2011. Building and destroying continental mantle. *Annual Review of Earth and Planetary Sciences* 39, 59–90.
- Marker, M., Knudsen, C., 1989. Middle Proterozoic ultramafic lamprophyre dykes in the Archaean of the Atã area, central West Greenland. *Rapport Grønlands Geologiske Undersøgelse* 145, 23–28.
- Marmo, J., Klemetti, M., Kinnunen, K., Lukkari, S., 2012. Avannaa Minibulk Piloting, Qeqertaa Ultramafic Lamprophyre. Report of investigation. GTK, Espoo, Finland, p. 44 (available by the senior author).
- Menzies, M.A., 1990. Archaean, Proterozoic, and Phanerozoic lithosphere. In: Menzies, M.A. (Ed.), *Continental Mantle*. Oxford University Press, Oxford, pp. 67–86.
- Mercier, J.-C., Nicolas, C.A., 1975. Textures and fabrics of upper-mantle peridotites as illustrated by xenoliths from basalts. *Journal of Petrology* 16 (2), 454–487.
- Negishi, H., Arai, S., Yurimoto, H., Ito, S., Ishimaru, S., Tamura, A., Akizawa, N., in press. Sulfide-rich dunite within a thick Moho transition zone of the northern Oman ophiolite: Implications for the origin of Cyprus-type sulfide deposits. *Lithos*.
- Nixon, P.H., Boyd, F.R., 1973. Petrogenesis of the granular and sheared ultrabasic nodule suite in kimberlites. In: Nixon, P.H. (Ed.), *Lesotho Kimberlites*. Lesotho National Development Corporation, Maseru, Lesotho, pp. 48–56.
- Nozaka, T., 2003. Compositional heterogeneity of olivine in thermally metamorphosed serpentinite from Southwest Japan. *American Mineralogist* 88, 1377–1384.
- O'Hara, M.J., Saunders, M.J., Mercy, E.L.P., 1975. Garnet–peridotite, primary ultrabasic magma and eclogite; interpretation of upper mantle processes in kimberlite. *Physics and Chemistry of the Earth* 9, 571–604.
- Oxburgh, E.R., Parmentier, E.M., 1977. Compositional and density stratification in oceanic lithosphere – causes and consequences. *Journal of the Geological Society of London* 133, 343–355.
- Oxburgh, E.R., Parmentier, E.M., Froidevaux, C., Harte, B., 1978. Thermal processes in the formation of continental lithosphere [and discussion]. *Philosophical Transactions of the Royal Society of London A* 288, 415–429.
- Pearson, D.G., Wittig, N., 2008. Formation of Archaean continental lithosphere and its diamonds: the root of the problem. *Journal of the Geological Society* 165, 895–914.
- Pearson, D.G., Canil, D., Shirey, S.B., 2003. Mantle samples included in volcanic rocks: xenoliths and diamonds. In: Holland, H.D., Turekian, K.K. (Eds.), *Treatise on Geochemistry*, volume 2. Elsevier, Amsterdam, pp. 171–275.
- Rudnick, R.L., McDonough, W.F., Orpin, A., 1994. Northern Tanzanian peridotite xenoliths: a comparison with Kaapvaal peridotites and inferences on metasomatic interactions. In: Meyer, H.O.A., Leonardos, O. (Eds.), *Kimberlites, related rocks and mantle xenoliths*, 1. CPRM, Brasília, Brazil, pp. 336–353.
- Sack, R.O., Ghiorso, M.S., 1991. Chromian spinels as petrogenetic indicators; thermodynamics and petrological applications. *American Mineralogist* 76, 827–847.
- Shirey, S.B., Walker, R.J., 1998. The Re–Os isotope system in cosmochemistry and high-temperature geochemistry. *Annual Review of Earth and Planetary Sciences* 26, 423–500.
- Stachel, T.J., Harris, W., Brey, G.P., 1998. Rare and unusual mineral inclusions in diamonds from Mwadui, Tanzania. *Contributions to Mineralogy and Petrology* 132, 34–47.
- Stripp, G.R., Field, M., Schumacher, J.C., 2006. Post-emplacement serpentization and related hydrothermal metamorphism in a kimberlite from Venetia, South Africa. *Journal of Metamorphic Geology* 24, 515–534.
- Suhr, G., Hellebrand, E., Snow, J.E., Seck, H.A., Hofmann, A.W., 2003. Significance of large, refractory dunite bodies in the upper mantle of the Bay of Island Ophiolite. *Geochemistry, Geophysics, Geosystems* 4, 1–34 (2001GC000277).
- Trommsdorff, V., López Sánchez-Vizcaino, V., Gómez-Pugnaire, M.T., Müntener, O., 1998. High pressure breakdown of antigorite to spinifex-textured olivine and orthopyroxene, SE Spain. *Contributions to Mineralogy and Petrology* 132, 139–148.
- Vance, J.A., Dungan, M.A., 1977. Formation of peridotites by deserpentinization in the Darrington and Sultan areas, Cascade Mountains, Washington. *Geological Society of America Bulletin* 88, 1497–1508.
- Walter, M.J., 1998. Melting of garnet peridotite and the origin of komatiite and depleted lithosphere. *Journal of Petrology* 39, 29–60.
- Walter, M.J., 2003. Melt extraction and compositional variability in mantle lithosphere. In: Holland, H.D., Turekian, K.K. (Eds.), *Treatise on Geochemistry*, vol. 2. Elsevier, pp. 363–394.
- Wittig, N., Pearson, D.G., Webb, M., Ottley, C.J., Irvine, G.J., Kopylova, M., Jensen, S.M., Nowell, G.M., 2008. Origin of cratonic lithospheric mantle roots: a geochemical study of peridotites from the North Atlantic Craton, West Greenland. *Earth and Planetary Science Letters* 274, 24–33.
- Wittig, N., Webb, M., Pearson, D.G., Dale, C.W., Ottley, C.J., Hutchinson, M., Jensen, S.M., Luguet, A., 2010. Formation of the North Atlantic Craton: timing and mechanisms constrained from Re–Os isotope and PGE data of peridotite xenoliths from S.W. Greenland. *Chemical Geology* 276, 166–187.